THE JOURNAL OF BIOLOGICAL CHEMISTRY VOL. 287, NO. 22, pp. 18210–18217, May 25, 2012
Published in the U.S.A.

Identification of Intercellular Cell Adhesion Molecule 1 (ICAM-1) as a Hypoglycosylation Marker in Congenital Disorders of Glycosylation Cells*[S]

Received for publication, February 22, 2012, and in revised form, April 6, 2012 Published, JBC Papers in Press, April 11, 2012, DOI 10.1074/jbc.M112.355677

Ping He[‡], Bobby G. Ng[‡], Marie-Estelle Losfeld[‡], Wenhong Zhu[§], and Hudson H. Freeze[‡1]

From the [‡]Genetic Disease Program, Sanford Children's Health Research Center, and the [§]National Cancer Institute Center Proteomics Facility, Sanford-Burnham Medical Research Institute, La Jolla, California 92037

Background: There are no general markers to detect hypoglycosylation and to test gene complementation in CDG cells.
Results: ICAM-1 expression is reduced in *N*-glycosylation-deficient cells and elevated when a normal gene is delivered to these cells.
Conclusion: ICAM-1 can be a useful cellular hypoglycosylation biomarker.
Significance: ICAM-1 can be used to confirm putative CDG gene defects and to test potential therapeutics for glycosylation-deficient cells.

Many human inherited disorders cause protein *N*-glycosylation defects, but there are few cellular markers to test gene complementation for such defects. Plasma membrane glycoproteins are potential biomarkers because they may be reduced or even absent in plasma membranes of glycosylation-deficient cells. We combined stable isotope labeling by amino acids in cell culture (SILAC) with linear ion trap mass spectrometry (LTQ Orbitrap^{TM}) to identify and quantify membrane proteins from wild-type CHO and glycosylation-deficient CHO (Lec9) cells. We identified 165 underrepresented proteins from 1447 unique quantified proteins, including 18 *N*-glycosylated plasma membrane proteins. Using various methods, we found that intercellular cell adhesion molecule 1 (ICAM-1) was reduced in Lec9 cells and in fibroblasts from 31 congenital disorder of glycosylation (CDG) patients compared with normal controls. Mannose supplementation of phosphomannose isomerase-deficient CDG-Ib (MPI-CDG) cells and complementation with *PMM2* in *PMM2*-deficient CDG-Ia (PMM2-CDG) cells partially corrected hypoglycosylation based on increased ICAM-1 presence on the plasma membrane. These data indicate that ICAM-1 could be a useful hypoglycosylation biomarker to assess gene complementation of CDG-I patient cells and to monitor improved glycosylation in response to therapeutic drugs.

Congenital disorders of glycosylation (CDG)[2] are caused by inherited genetic defects in *N*-linked glycosylation (1). This results in unoccupied glycosylation sites (type I) or altered processing of protein-bound sugar chains (type II). Mutations in over 35 genes in the *N*-glycosylation pathway are thought to affect >1000 patients, but the actual number of patients and distinct disorders is probably much higher. Patients exhibit highly variable motor and intellectual disabilities, seizures, developmental delays, hypoglycemia, and clotting and digestion abnormalities (2).

Serum transferrin is a widely used marker to initially identify *N*-glycosylation-deficient patients based on the absence or abnormality of the attached sugar chains. However, transferrin does not detect all *N*-glycosylation defects (3) and does not pinpoint the defective gene (4). More important, there is currently no corresponding indicator of reduced glycosylation in patient cells. Having such a marker would be useful to test potential therapeutics in glycosylation-deficient cells by restoring *N*-glycosylation of the marker. A marker could also be used to test gene complementation in glycosylation-deficient cells. This would be an important tool to verify candidate defective genes identified by whole exome sequencing.

Proteins with unoccupied glycosylation sites are often degraded by glycoprotein quality control mechanisms (5) and fail to reach the plasma membrane. Such proteins might show lower expression in glycosylation-deficient cells and could be potential markers of hypoglycosylation. We applied quantitative proteomics to profile and quantify membrane proteins from wild-type CHO cells (Pro5) and Lec9 CHO cells, which have a defect in the synthesis of dolichol, a critical lipid needed for *N*-glycosylation (6). We found lower levels of intercellular cell adhesion molecule 1 (ICAM-1) in Lec9 cells. We extended this to a series of 31 type I CDG fibroblasts and verified ICAM-1 as a potential hypoglycosylation biomarker for gene complementation and therapeutic improvement.

EXPERIMENTAL PROCEDURES

Materials—Most of the reagents were purchased from Sigma-Aldrich. α-Minimal essential medium and DMEM with and without glucose were obtained from Mediatech, Inc. (Manassas, VA). FBS was obtained from HyClone Laboratories (Logan, UT). SILAC^{TM} protein identification quantitation kits,

* This work was supported, in whole or in part, by National Institutes of Health Grant R01 DK55615. This work was also supported by the Rocket Fund.
[S] This article contains supplemental Fig. 1 and Table 1.
[1] To whom correspondence should be addressed: Sanford-Burnham Medical Research Institute, 10901 North Torrey Pines Rd., La Jolla, CA 92037. Tel.: 858-646-3142; Fax: 858-713-6281; E-mail: hudson@sanfordburnham.org.
[2] The abbreviations used are: CDG, congenital disorder(s) of glycosylation; ICAM-1, intercellular cell adhesion molecule 1; Bis-Tris, 2-[bis(2-hydroxyethyl)amino]-2-(hydroxymethyl)propane-1,3-diol; SILAC, stable isotope labeling by amino acids in cell culture; IF, immunofluorescence.

NuPAGE Novex Bis-Tris mini gels, and Alexa Fluor 488- and Alexa Fluor 647-conjugated secondary antibodies were purchased from Invitrogen (Carlsbad, CA). Anti-integrin α5 polyclonal antibody was purchased from Millipore (Bedford, MA). Goat anti-mouse ICAM-1 antibody was purchased from R&D Systems (Minneapolis, MN). FITC-conjugated anti-human CD54 (ICAM-1) antibody was purchased from BioLegend (San Diego, CA). Alexa 647-conjugated anti-FLAG antibody was purchased from Cell Signaling Technology (Danvers, MA). Phycoerythrin-conjugated mouse anti-human CD54 (ICAM-1) antibody was a kind gift from Vasileios Bekiaris in Dr. Carl Ware's laboratory (Sanford-Burnham Medical Research Institute). Horseradish peroxidase-conjugated secondary antibodies were purchased from Jackson ImmunoResearch Laboratories (West Grove, PA). Pierce ECL Western blotting substrate was purchased from Thermo Scientific (Wilmington, DE). WesternBright Quantum was obtained from Advansta (Menlo Park, CA). An Immun-Star WesternC kit was purchased from Bio-Rad. Nitrocellulose membrane was purchased from Whatman (Dassel, Germany). Eight-chamber tissue culture-treated glass slides were purchased from BD Biosciences.

Cell Culture—Wild-type CHO cells (Pro5) and CHO cells with a genetic defect in dolichol synthesis (Lec9) were maintained in α-minimal essential medium supplemented with 10% FBS. Normal and CDG patient fibroblasts were cultured in DMEM (with 1 g/liter glucose) with 10% FBS. HeLa cells were maintained in DMEM (with 4.5g/liter glucose) and 10% FBS. All cells were maintained in the recommended media at 37 °C and 5% CO_2.

Stable Isotope Labeling by Amino Acids in Cell Culture (SILAC)—The Pro5 and Lec9 cells were labeled by isotope as recommended in the SILAC kit instructions. Briefly, heavy L-[U-$^{13}C_6$]lysine and light L-[U-$^{12}C_6$]lysine were added to RPMI 1640 medium with 10% dialyzed FBS, which was used to culture Lec9 (heavy) and Pro5 (light) cells for six doubling times (~4 days) at 37 °C and 5% CO_2.

Membrane Preparation—Approximately 2.5×10^6 Pro5 and Lec9 cells grown as described above were mixed at a 1:1 ratio. Extraction of membrane proteins were done according to the manufacturer's protocol.

Protein Analysis by Two-dimensional LC-MS/MS—SILAC-labeled membrane pellet was resuspended in 50 mM ammonium bicarbonate and digested in methanol/water solution according to a previously reported protocol (7). Briefly, after the addition of 50 mM ammonium bicarbonate, the sample was incubated at 90 °C for 20 min, cooled, and diluted with methanol to yield a 60% (v/v) solution. Proteins were digested with trypsin overnight at 37 °C, and the solution was evaporated in a SpeedVac concentrator. The peptides were redissolved in 200 μl of 95% buffer containing 5% acetonitrile and 0.1% formic acid and 5% buffer containing 25% acetonitrile, 0.1% formic acid, and 500 mM KCl. Peptides were first separated by strong cation exchange HPLC with a PolySULFOETHYL A™ column (Michrom Bioresources, Inc., Auburn, CA). Twelve strong cation exchange fractions were collected and subjected to reverse-phase LC-MS/MS analysis using a Paradigm HPLC Magic C18 column (0.2 × 150 mm; Michrom Bioresources, Inc.) and an LTQ Orbitrap™ XL mass spectrometer (Thermo Scientific). The peptides were separated by 60–120 min of 5–40% buffer containing 100% acetonitrile and 0.1% formic acid, and spectra were collected in a data-dependent mode. Each scan was set to acquire a full MS scan, followed by MS/MS scans on the four most intense precursor ions.

Data Analysis and Quantification—Functional classifications were performed with Gene Ontology annotation. Both the protein identification and the SILAC quantification were performed using IP2 v1.01 (Integrated Proteomics Applications, San Diego, CA). First, MS1 and MS2 files were extracted by RawExtractor v1.9 (The Scripps Research Institute, La Jolla, CA). The genomic sequence of the CHO-K1 cell line was published recently (8), and the data were not accessible when we performed the protein identification. Therefore, a database including the International Protein Index mouse database (v3.73) plus ~500 available Chinese hamster proteins was uploaded into IP2, which automatically generated a reverse protein database. The MS1 and MS2 files were searched using ProLuCID and the decoy database, with 50 ppm precursor mass tolerance and semitryptic specificity. Variable modifications included 16 Da on methionine and 6 Da on lysine. At least two peptides were required for each protein. The DTASelect parameters were carefully set so that the final false positive rate was 1.77%, and the false positive rate at the peptide level was 1.01%. Quantification analysis was then selected for SILAC, and the protein ratios and S.D. were calculated by Census on IP2. We also performed the data analysis using the recently published CHO-K1 genome database. The results were very similar, and all of the previously established marker candidates were still in the identification list.

SDS-PAGE and Western Blotting—SDS-PAGE and Western blotting were carried out as described by Jones *et al.* (9). For detection of ICAM-1 in human fibroblasts, ECL substrate with higher sensitivity (WesternBright Quantum) or an Immun-Star WesternC kit was used. The images were captured either by film exposure or with a Bio-Rad CCD imaging system. The gray intensity was calculated using Image Lab 3.0.1 (Beta 2) software (Bio-Rad).

ICAM-1 Immunofluorescence (IF) Staining—The protocol was adapted from Peanne *et al.* (10) by adding 4% sucrose to paraformaldehyde in fixation buffer.

Flow Cytometry (FACS)—Cell surface ICAM-1 staining was performed as described by Srikrishna *et al.* (11). The cell surface and intracellular protein staining was described elsewhere (12). Flow cytometry was performed with a BD Biosciences FACSCalibur analyzer and analyzed with CellQuest Pro software. The mean fluorescence after subtracting the background using IgG reflected only the level of cell surface ICAM-1.

Mannose Supplementation Assay—CDG-Ib cells were cultured to 70–80% confluence, followed by the addition of 25–200 μM mannose in culture medium and incubation at 37 °C for 24 h.

Gene Complementation—The *PMM2* (phosphomannomutase-2) complementation was done as described by Jones *et al.* (9), except that PMM2 was tagged with FLAG (DYKDDDDK) at the N terminus.

PMM2 Enzyme Assays—PMM2 enzyme assays were performed as described by Sharma *et al.* (13).

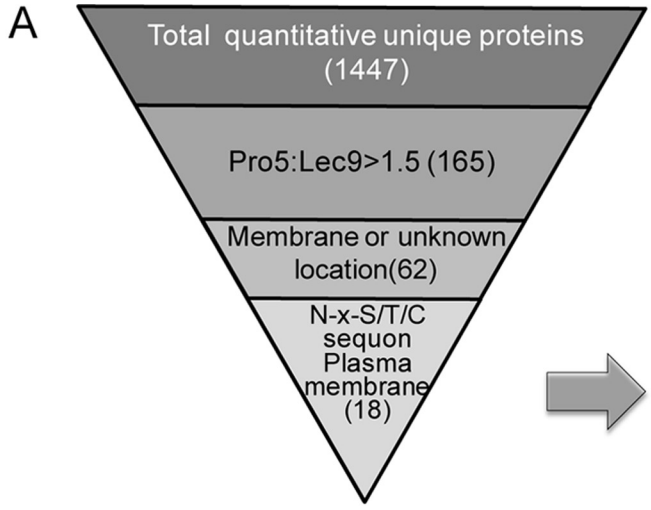

Protein	average ratio (pro5:lec9)	st dev	peptide num
Intercellular adhesion molecule 1 (ICAM-1)	2.52	0.18	3
Bone marrow stromal antigen 2	2.35		1
Plasma membrane calcium-transporting ATPase 2	2.18		1
Multidrug resistance protein 2	1.83		1
Desmoyokin	1.82	0.11	15

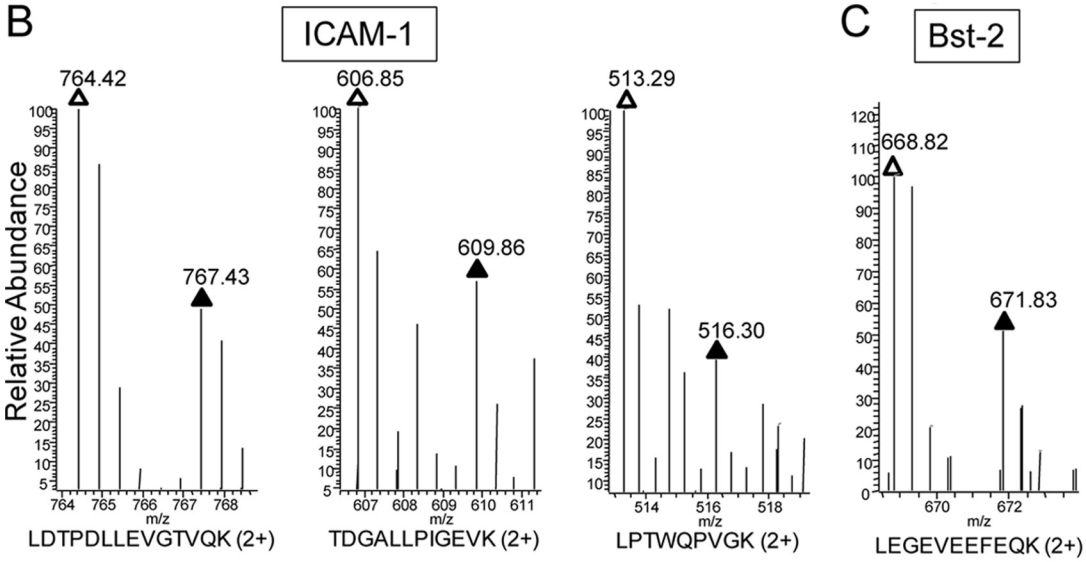

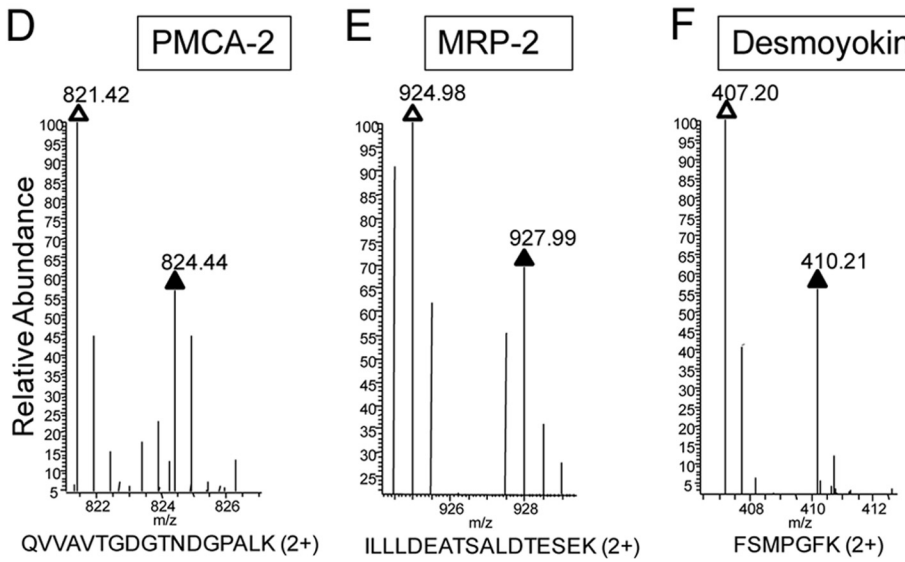

FIGURE 1. *A*, refinement of marker candidates. To identify the potential hypoglycosylated markers, the following criteria were applied to refine the candidate list: 1) >1.5-fold underrepresented in Lec9 cells compared with Pro5 cells (from 1447 to 165), 2) cell membrane or unknown localization by Gene Ontology annotation analysis (from 165 to 62), 3) plasma membrane protein with NX(S/T) *N*-glycosylation sequons (from 62 to 18), and 4) protein with high quality raw spectral data and a commercial antibody available. *st dev*, standard deviation; *num*, number. *B–F*, SILAC peptide pairs of ICAM-1, Bst-2, PMCA2, MRP2, and desmoyokin, respectively. *White* and *black triangles* represent peptides from Pro5 and Lec9 cells, respectively.

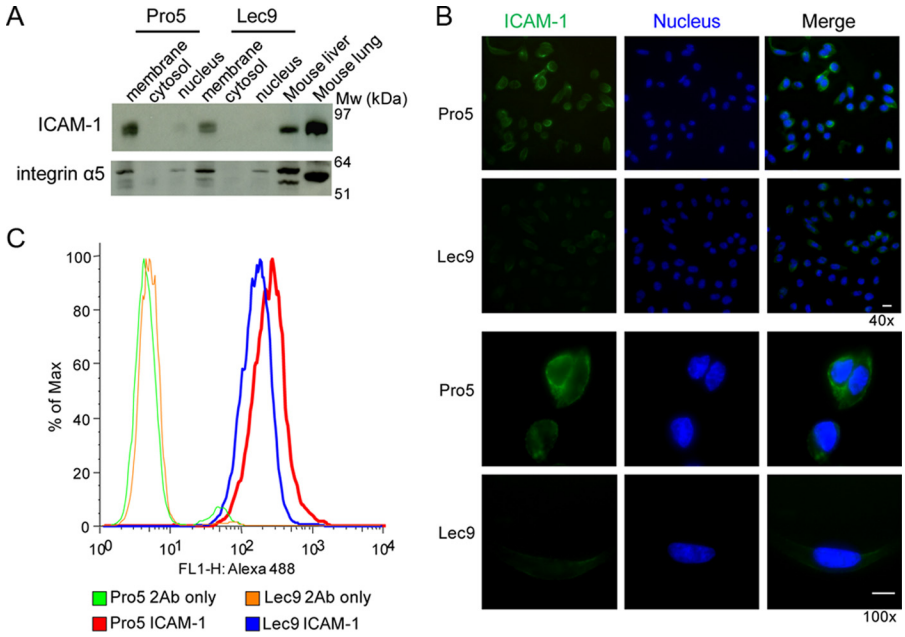

FIGURE 2. **Validation of ICAM-1 underrepresented in Lec9 cells compared with Pro5 cells.** *A*, Western blot analysis of ICAM-1 levels in Pro5 and Lec9 cells after subcellular fractionation. Integrin α5 was used as a membrane fraction marker, and mouse liver and lung extract was used as a positive control for ICAM-1. *B*, IF staining of ICAM-1 in Pro5 and Lec9 cells. The cells were first fixed and blocked and then incubated with anti-mouse ICAM-1 primary antibody, followed by incubation with Alexa Fluor 488-conjugated secondary antibody. The nuclei were stained with DAPI. The displayed images are the overlay of *green* (ICAM-1) and *blue* (nucleus) channels. *Scale bars* = 10 μm. *C*, ICAM-1 expression histogram by FACS analysis. The resuspended cells were stained with or without anti-human ICAM-1 antibody, followed by incubation with Alexa Fluor 488-conjugated secondary antibodies.

Statistics—An unpaired *t* test was used to compare means between two groups, and $p < 0.05$ was considered statistically significant.

RESULTS

Underrepresented Membrane Proteins in Lec9 Cells—SILAC is a well established, quantitative method to determine protein relative abundance between samples (14–16). We combined SILAC with linear ion trap MS (LTQ Orbitrap) to identify and quantify membrane proteins from wild-type CHO cells (Pro5) and CHO cells with a defect in dolichol synthesis (Lec9) (6). The Pro5 and Lec9 cells were labeled with light and heavy L-lysine, respectively. After six doublings, both cell lines were mixed equally, followed by membrane protein extraction, two-dimensional LC-MS/MS analysis, and data analysis. A total of 3775 quantified peptides were assigned to 1447 unique proteins in the membrane fraction. We compared the relative abundance of these membrane proteins between the two CHO cell lines by calculating the ratios of intensities of the corresponding SILAC peptide pairs (supplemental Table 1). As expected, the protein ratios clustered tightly around 1:1 (proteins with a 0.67–1.5-fold difference account for 84%), indicating that most of the membrane proteins in both cell lines are expressed at the same level. Furthermore, the majority (93%) of the 165 underrepresented (>1.5-fold) proteins are 1.5–3-fold reduced in Lec9 cells.

To identify potential hypoglycosylated glycoproteins, we used a serial slimming strategy to cull the candidates as follows (Fig. 1*A*): 1) 165 proteins >1.5-fold underrepresented in Lec9 cells compared with Pro5 cells, 2) 62 proteins with cell surface or unknown localization by Gene Ontology annotation analysis, and 3) 18 plasma membrane proteins with N*X*(S/T) *N*-glycosylation sequons that are highlighted in supplemental Table 1. These were further narrowed to five candidates based on quality of the raw spectral data and availability of commercial antibodies. These included ICAM-1, Bst-2 (bone marrow stromal antigen 2), PMCA2 (plasma membrane calcium-transporting ATPase 2), MRP2 (multidrug resistance protein 2), and desmoyokin. The representative raw spectra of the SILAC peptide pairs of these candidates are displayed in Fig. 1 (*B*–*F*), in which the difference in protein levels between Pro5 and Lec9 cells ranged from 1.8- to 2.5-fold. Among the list of candidates, ICAM-1 showed the largest protein expression ratio difference (2.52) calculated by three quantitative peptide pairs between Pro5 and Lec9 cells and a relative low S.D. (0.18; coefficient of variation of 7%).

ICAM-1 expression was first examined by a series of biochemical experiments. ICAM-1 is a transmembrane protein with five extracellular Ig-like domains and nine occupied *N*-glycosylation sites in CHO cells (17). It is constitutively expressed by epithelial cells and normally expressed at low levels on immune system and endothelial cells, but it is dramatically upregulated in response to inflammatory stimuli (18, 19). As shown by SILAC quantitative peptide pairs in Fig. 1*B*, ICAM-1 was expressed nearly 2.5-fold higher in the membrane fraction of Pro5 cells compared with Lec9 cells, which was supported by Western blotting (Fig. 2*A*), IF staining (Fig. 2*B*), and flow cytometry analysis (Fig. 2*C*).

We also used Western blot analysis (supplemental Fig. 1) to check the expression of Bst-2, PMCA2, and MRP2 in Pro5 and Lec9 cells and in several CDG patient cells, yet they were expressed only in trace amounts, making them less reliable than ICAM-1. The desmoyokin antibody was not available. Therefore, the subsequent analysis focused on ICAM-1.

Reduced ICAM-1 Is Detected in CDG Patient Fibroblasts—On the basis of the CHO cell results, we predicted that CDG patient fibroblast cell lines would have reduced ICAM-1 compared with controls. We measured ICAM-1 expression in seven controls and 31 CDG patient cell lines with proven or unknown genetic defects that produce proteins with unoccupied glycosylation sites (type I CDG). The specific genes and the number of patients analyzed are listed in Table 1.

TABLE 1
Glycosylation genes and number of patients analyzed

Sample	Defect	Cases
Control	None	7
Ia	*PMM2*	7
Ib	*MPI*	4
Ik	*ALG1*	6
Unknown	Undefined	14
Total		**38**

We first detected ICAM-1 on the cell surface by FACS analysis (Fig. 3*A*). Relative mean fluorescence calculation (Fig. 3*E*, *left panel*) demonstrated that ICAM-1 was underrepresented or completely absent in CDG patient fibroblasts ($p = 0.0007$). IF staining results are consistent with FACS data (Fig. 3*D*). Furthermore, membrane proteins were extracted from some CDG-Ia, CDG-Ib, and control fibroblasts, and ICAM-1 expression was analyzed by Western blotting. ICAM-1 was barely expressed in the vast majority of CDG patient fibroblasts compared with control cells (Fig. 3*B*), in agreement with the results of FACS analysis (Fig. 3*A*). Because ICAM-1 was found mainly in the membrane fraction by Western blot analysis (Fig. 3*B*) and on the fibroblast cell surface by IF staining (Fig. 3*D*), we reasoned that Western blot analysis of the total lysate would also reflect ICAM-1 expression at the cell surface. This was confirmed by showing that ICAM-1 expression was

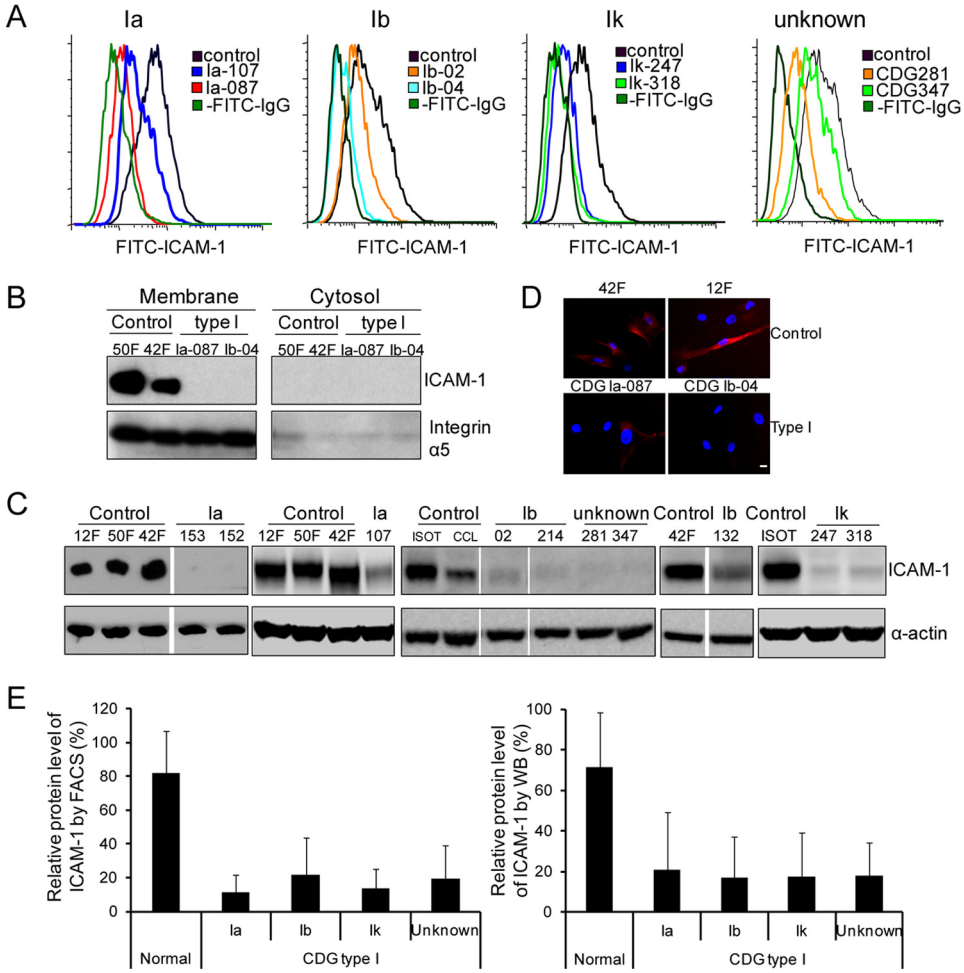

FIGURE 3. **Validation of reduced ICAM-1 in CDG patient fibroblasts.** *A*, representative cell surface ICAM-1 expression histogram of control, CDG-Ia, CDG-Ib, and CDG-Ik fibroblasts and fibroblasts from patients with an undefined genetic defect by FACS analysis. Cells were stained with or without FITC-conjugated anti-human ICAM-1 antibodies. The *numbers* (*e.g.* 107, 087, etc.) indicate in-house patient identification numbers. *B* and *C*, representative Western blot analysis of ICAM-1 expression in control and CDG patient fibroblasts. *B*, proteins in the membrane fraction were analyzed. Integrin α5 served as both a membrane fraction marker and a loading control. *C*, total lysate was analyzed, and the control of gel loading is shown with anti-α-actin staining. *D*, IF staining of ICAM-1 in fibroblasts. The cells were stained with phycoerythrin-conjugated anti-mouse ICAM-1 primary antibody. The displayed images are the overlay of *red* (ICAM-1) and *blue* (nucleus) channels. *Scale bar* = 10 μm. *E*, relative levels of ICAM-1. The *left panel* is based on the calculation of FACS data. The ICAM-1 level was first calculated as the mean fluorescence minus the background (without staining with anti-ICAM-1 antibodies). In each assay, the ICAM-1 mean fluorescence value of each cell was divided by that of the control to give the relative value for each type of fibroblast as a percentage of the control. The *right panel* is based on the calculation of Western blot (*WB*) data derived from both membrane and total protein analyses. The gray intensity of ICAM-1 was divided by that of the loading control (integrin α5 for membrane protein or α-actin for total protein) to normalize the ICAM-1 level. In each assay, the normalized ICAM-1 value of each cell was divided by that of the control to obtain the relative value for each type of fibroblast. Each assay was repeated at least twice, and the values are the average of four to seven individual fibroblasts. Each *error bar* in the histogram represents the S.D. of various individuals in each group.

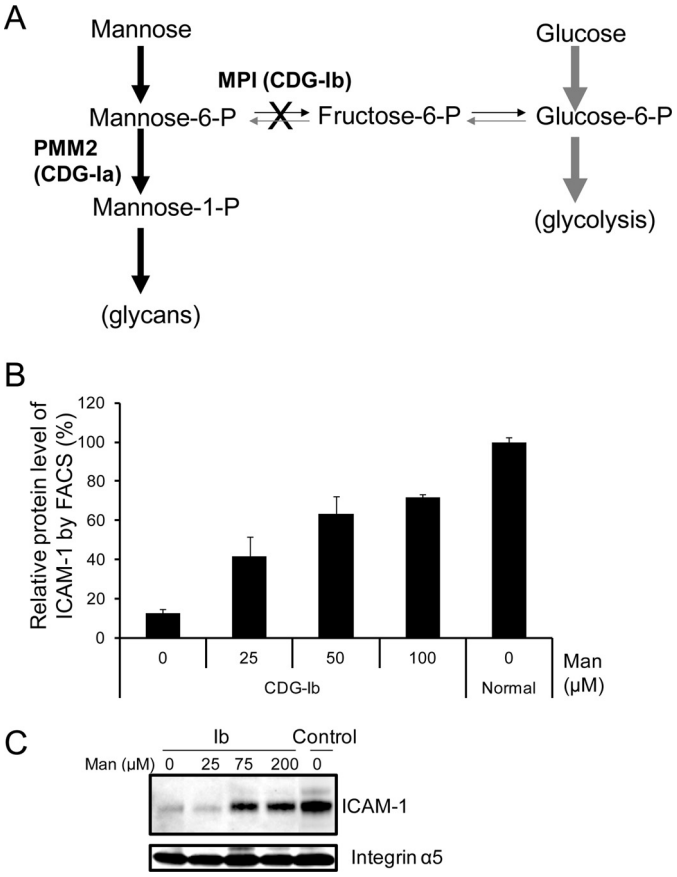

FIGURE 4. **Mannose supplementation increases amount of ICAM-1 and its appearance on cell surface of CDG-Ib cells.** *A*, mannose supplementation as a therapeutic in CDG-Ib. The supplemented mannose enhances flux through the complementary metabolic pathway, which partially corrects Man-6-P deficiency due to deficient phosphomannose isomerase (*PMI*) activity and in turn fuels more glycan synthesis. *B*, FACS analysis of ICAM-1 alteration on the CDG-Ib cell surface when supplemented with increased amounts of mannose. CDG-Ib cells were treated with increasing amounts of mannose (25–100 μM) for 24 h. The cells were stained with phycoerythrin-conjugated anti-human ICAM-1 antibodies. Each *error bar* in the histogram represents the mean ± S.D. of duplicate determinations of independent experiments. *C*, Western blot analysis of ICAM-1 expression in CDG-Ib membranes when supplemented with increased amounts of mannose. CDG-Ib cells were treated with increasing amounts of mannose (25–200 μM) for 24 h. Membrane proteins were extracted and analyzed. Integrin α5 served as both a membrane fraction marker and a loading control.

significantly reduced in type I CDG fibroblasts compared with control cells ($p = 0.0023$) (Fig. 3, *C* and *E*, *right panel*).

Of note, two samples (Ia-107 and Ib-132) did not show reduced expression as dramatic as that seen in other CDG cells (Fig. 3*C*). Patient Ia-107 is a clinically very mild case and has ~34% residual PMM2 activity. However, FACS analysis showed that ICAM-1 expression is reduced by 66% in Ia-107 (Fig. 3*A*) and by 35% in Ib-132 compared with the average in control fibroblasts.

Mannose Supplementation Increases Cell Surface ICAM-1 in CDG-Ib Cells—CDG-Ib (MPI-CDG) is caused by mutations in *PMI*, encoding phosphomannose isomerase, which converts Fru-6-P to Man-6-P (20). CDG-Ib patients and their cells improve glycosylation when given mannose supplements by restoring Man-6-P through a complementary metabolic pathway (Fig. 4*A*). We supplemented CDG-Ib cells with increasing amounts of mannose (25–200 μM) for 24 h, which increased cell surface ICAM-1 expression as detected by FACS analysis (Fig. 4*B*) and Western blotting (Fig. 4*C*). Increasing mannose did not change ICAM-1 levels in control fibroblasts (data not shown), indicating that mannose therapy partially corrects ICAM-1 hypoglycosylation and allows newly synthesized, glycosylated ICAM-1 delivery to the plasma membrane. The data presented here illustrate that ICAM-1 can be used as an indicator to reflect a glycosylation therapeutic response for patient cells.

PMM2 Complementation Increases ICAM-1 Levels on CDG-Ia Fibroblast Surface—CDG-Ia (PMM2-CDG) is the most prevalent CDG type and is caused by mutations in *PMM2*, encoding phosphomannomutase-2, which converts Man-6-P to Man-1-P. Three CDG-Ia patient fibroblast lines were infected with recombinant retroviruses expressing the wild-type *PMM2* cDNA containing a FLAG tag or an empty vector. The complementation successfully corrected the *PMM2* deficiency in these CDG-Ia fibroblasts as shown by a nearly 6-fold increase in PMM2 activity in the complemented cells compared with the non-complemented cells (Fig. 5*A*). We then examined cellular ICAM-1 expression in control cells, CDG-Ia cells, and CDG-Ia cells infected with an empty vector or a vector containing *PMM2* by FACS analysis. We found an ~2.5-fold increase in ICAM-1 in *PMM2*-transfected CDG-Ia cells compared with vector-transfected cells, in which the ICAM-1 level in the complemented cells reached over half of that in the control cells (Fig. 5*B*). Of note, ICAM-1 also increased when the empty vector was used (Fig. 5*B*) (21, 22). To determine whether the ICAM-1 level is positively correlated with the amount of wild-type *PMM2* delivered, patient fibroblasts were gated at high and low FLAG-PMM2 levels (Fig. 5*C*, *left panel*). A >4-fold increase in ICAM-1 was observed on the surface of high level FLAG-PMM2 cells compared with the low level population, and the ICAM-1 level in the complemented cells reached nearly 70% of that in the control cells (Fig. 5*C*, *middle* and *right panels*). Our results clearly show that complementation with wild-type *PMM2* functionally corrected *PMM2* deficiency and correspondingly increased ICAM-1 expression on the cell surface. Therefore, ICAM-1 can clearly detect hypoglycosylation and show its improvement in response to gene correction.

DISCUSSION

Patients with inherited glycosylation disorders have multiple glycosylation-deficient serum/plasma glycoproteins. However, there are no reliable glycosylation markers available in patient fibroblasts. As most cell surface proteins are glycosylated, they might be at risk of destruction in glycosylation-deficient cells. We hypothesized that some hypoglycosylated proteins could also fail to localize to the plasma membrane because the misfolded proteins would be degraded by endoplasmic reticulum-associated degradation (23). Hence, plasma membrane proteins could be considered as biomarker candidates for impaired glycosylation (24). Besides the serum glycoproteins such as transferrin, some membrane-associated glycoproteins might serve as alternative indicators of a glycosylation defect (4). However, the published data have focused mainly on the alteration of glycan structure rather than glycosylation site occupancy (25–27). Some CDG patient cell lines show underglyco-

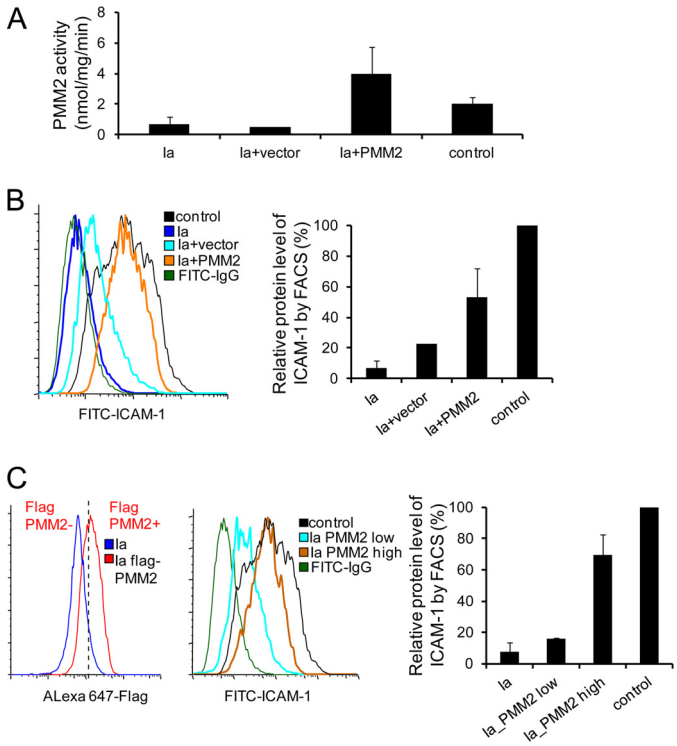

FIGURE 5. **Correction of *PMM2* deficiency in CDG-Ia patient fibroblasts by retroviral *PMM2* gene delivery.** *A*, PMM2 activity. PMM2 activity was measured in CDG-Ia fibroblasts ($n = 3$), CDG-Ia fibroblasts with empty vector ($n = 1$), CDG-Ia fibroblasts with wild-type *PMM2* ($n = 3$), and control fibroblasts ($n = 2$). Each *error bar* in the histogram represents the S.D. of data from multiple experiments for two or three individuals. *B*, representative cell surface ICAM-1 expression histogram of control ($n = 1$), CDG-Ia ($n = 2$), and *PMM2*-complemented fibroblasts ($n = 2$) by FACS analysis (*left panel*). The *right panel* shows the calculation of FACS data. *C*, representative cell surface ICAM-1 expression histogram of *PMM2*-complemented CDG-Ia fibroblasts ($n = 2$) according to the exogenous FLAG-PMM2 level by FACS analysis (*left panel*). The cells were fixed and permeabilized, followed by staining with anti-FLAG antibodies. In the FACS analysis, fibroblasts infected with viruses expressing *PMM2* cDNA with a FLAG tag were gated into high and low level PMM2 groups, and the mean level of ICAM-1 fluorescence in each group was calculated. The ICAM-1 mean fluorescence value of each group of cells was divided by that of the controls to give the relative value as a percentage of the control. Each assay was repeated at least twice, and the values are the average of two individual fibroblasts. Each *error bar* in the histogram represents the S.D. of data from multiple experiments for individuals in each group.

sylation of adenovirus-transfected DNase I (28, 29), but those results are inconsistent and not easily applied to routine examination.

Protein hypoglycosylation in type I CDG patients results from the defects in synthesis or transfer of lipid-linked oligosaccharide glycan to protein. This in turn may result in protein misfolding/unfolding, degradation by the proteasome, and absence from the plasma membrane. For this reason, we selected type I CDG fibroblasts to test the expression of marker candidates. We detected reduced ICAM-1 in 29 of 31 of these type I CDG cell lines (94%) with known or undefined genetic defects that cause hypoglycosylation (Fig. 3). Two cell lines with very mild enzymatic deficiencies showed only slight (<2-fold) decreases in ICAM-1 levels.

More ICAM-1 localized on the cell surface when CDG-Ib cells were supplemented with mannose (Fig. 4), indicating that ICAM-1 could be an indicator of therapeutics for improved glycosylation. *PMM2* complementation in CDG-Ia cells increased ICAM-1 expression on the patient fibroblast surface (Fig. 5), supporting the utility of ICAM-1 to confirm the putative defective genes by complementation.

We used systematic quantitative proteomics to establish potential hypoglycosylation markers under stringent criteria. ICAM-1 proved to be decreased on the cell surface in CDG patient fibroblasts. Mannose supplementation of CDG-Ib cells and *PMM2* cDNA complementation of CDG-Ia cells partially corrected hypoglycosylation, allowing ICAM-1 to "reappear" on the plasma membrane. Our data indicate that ICAM-1 could be a useful hypoglycosylation biomarker for type I CDG cells, but we are also exploring whether ICAM-1 is decreased in type II CDG cells as well.

Acknowledgments—We are indebted to Khatereh Motametchaboki for help in coordinating the quantitative proteomic analysis. We thank Kutbuddin Doctor for the analysis of N-glycosylation sites in the identified proteins. We also appreciate the generosity of Vasileios Bekiaris for providing phycoerythrin-conjugated anti-human ICAM-1 antibodies. We thank Geetha Srikrishna and Vandana Sharma for constructive comments during the writing of this manuscript.

REFERENCES

1. Freeze, H. H., and Sharma, V. (2010) Metabolic manipulation of glycosylation disorders in humans and animal models. *Semin. Cell Dev. Biol.* **21,** 655–662
2. Freeze, H. H. (2007) Congenital disorders of glycosylation: CDG-I, CDG-II, and beyond. *Curr. Mol. Med.* **7,** 389–396
3. Westphal, V., Xiao, M., Kwok, P. Y., and Freeze, H. H. (2003) Identification of a frequent variant in *ALG6*, the cause of congenital disorder of glycosylation Ic. *Hum. Mutat.* **22,** 420–421
4. Marklová, E., and Albahri, Z. (2007) Screening and diagnosis of congenital disorders of glycosylation. *Clin. Chim. Acta* **385,** 6–20
5. Ellgaard, L., and Helenius, A. (2001) ER quality control: towards an understanding at the molecular level. *Curr. Opin. Cell Biol.* **13,** 431–437
6. Rosenwald, A. G., and Krag, S. S. (1990) Lec9 CHO glycosylation mutants are defective in the synthesis of dolichol. *J. Lipid Res.* **31,** 523–533
7. Blonder, J., Goshe, M. B., Moore, R. J., Pasa-Tolic, L., Masselon, C. D., Lipton, M. S., and Smith, R. D. (2002) Enrichment of integral membrane proteins for proteomic analysis using liquid chromatography-tandem mass spectrometry. *J. Proteome Res.* **1,** 351–360
8. Xu, X., Nagarajan, H., Lewis, N. E., Pan, S., Cai, Z., Liu, X., Chen, W., Xie, M., Wang, W., Hammond, S., Andersen, M. R., Neff, N., Passarelli, B., Koh, W., Fan, H. C., Wang, J., Gui, Y., Lee, K. H., Betenbaugh, M. J., Quake, S. R., Famili, I., and Palsson, B. O. (2011) The genomic sequence of the Chinese hamster ovary (CHO)-K1 cell line. *Nat. Biotechnol.* **29,** 735–741
9. Jones, M. A., Ng, B. G., Bhide, S., Chin, E., Rhodenizer, D., He, P., Losfeld, M. E., He, M., Raymond, K., Berry, G., Freeze, H. H., and Hegde, M. R. (2012) *DDOST* mutations identified by whole exome sequencing are implicated in congenital disorders of glycosylation. *Am. J. Hum. Genet.* **90,** 363–368
10. Peanne, R., Legrand, D., Duvet, S., Mir, A. M., Matthijs, G., Rohrer, J., and Foulquier, F. (2011) Differential effects of lobe A and lobe B of the conserved oligomeric Golgi complex on the stability of β1,4-galactosyltransferase 1 and α2,6-sialyltransferase 1. *Glycobiology* **21,** 864–876
11. Srikrishna, G., Turovskaya, O., Shaikh, R., Newlin, R., Foell, D., Murch, S., Kronenberg, M., and Freeze, H. H. (2005) Carboxylated glycans mediate colitis through activation of NF-κB. *J. Immunol.* **175,** 5412–5422
12. Schmid, I., Uittenbogaart, C. H., and Giorgi, J. V. (1991) A gentle fixation and permeabilization method for combined cell surface and intracellular staining with improved precision in DNA quantification. *Cytometry* **12,** 279–285

13. Sharma, V., Ichikawa, M., He, P., Scott, D. A., Bravo, Y., Dahl, R., Ng, B. G., Cosford, N. D., and Freeze, H. H. (2011) Phosphomannose isomerase inhibitors improve *N*-glycosylation in selected phosphomannomutase-deficient fibroblasts. *J. Biol. Chem.* **286,** 39431–39438
14. Ong, S. E., Blagoev, B., Kratchmarova, I., Kristensen, D. B., Steen, H., Pandey, A., and Mann, M. (2002) Stable isotope labeling by amino acids in cell culture, SILAC, as a simple and accurate approach to expression proteomics. *Mol. Cell. Proteomics* **1,** 376–386
15. Prokhorova, T. A., Rigbolt, K. T., Johansen, P. T., Henningsen, J., Kratchmarova, I., Kassem, M., and Blagoev, B. (2009) Stable isotope labeling by amino acids in cell culture (SILAC) and quantitative comparison of the membrane proteomes of self-renewing and differentiating human embryonic stem cells. *Mol. Cell. Proteomics* **8,** 959–970
16. Zhang, G., Deinhardt, K., Chao, M. V., and Neubert, T. A. (2011) Study of neurotrophin-3 signaling in primary cultured neurons using multiplex stable isotope labeling with amino acids in cell culture. *J. Proteome Res.* **10,** 2546–2554
17. Otto, V. I., Damoc, E., Cueni, L. N., Schürpf, T., Frei, R., Ali, S., Callewaert, N., Moise, A., Leary, J. A., Folkers, G., and Przybylski, M. (2006) *N*-Glycan structures and *N*-glycosylation sites of mouse soluble intercellular adhesion molecule 1 revealed by MALDI-TOF and FTICR mass spectrometry. *Glycobiology* **16,** 1033–1044
18. Pino, M., Galleguillos, C., Torres, M., Sovino, H., Fuentes, A., Boric, M. A., and Johnson, M. C. (2009) Association between MMP1 and MMP9 activities and ICAM-1 cleavage induced by tumor necrosis factor in stromal cell cultures from eutopic endometria of women with endometriosis. *Reproduction* **138,** 837–847
19. Horikoshi, T., Ezoe, K., Nakagawa, H., Eguchi, H., Hanada, N., and Hamaoka, S. (1995) Up-regulation of ICAM-1 expression on human dermal fibroblasts by IFN-β in the presence of TNF-α. *FEBS Lett.* **363,** 141–144
20. Freeze, H. H. (2006) Genetic defects in the human glycome. *Nat. Rev. Genet.* **7,** 537–551
21. Papi, A., and Johnston, S. L. (1999) Rhinovirus infection induces expression of its own receptor intercellular adhesion molecule 1 (ICAM-1) via increased NF-κB-mediated transcription. *J. Biol. Chem.* **274,** 9707–9720
22. Dhawan, S., Puri, R. K., Kumar, A., Duplan, H., Masson, J. M., and Aggarwal, B. B. (1997) Human immunodeficiency virus 1 Tat protein induces the cell surface expression of endothelial leukocyte adhesion molecule 1, vascular cell adhesion molecule 1, and intercellular adhesion molecule 1 in human endothelial cells. *Blood* **90,** 1535–1544
23. Smith, M. H., Ploegh, H. L., and Weissman, J. S. (2011) Road to ruin: targeting proteins for degradation in the endoplasmic reticulum. *Science* **334,** 1086–1090
24. Roth, J. (2002) Protein *N*-glycosylation along the secretory pathway: relationship to organelle topography and function, protein quality control, and cell interactions. *Chem. Rev.* **102,** 285–303
25. Van Geet, C., Jaeken, J., Freson, K., Lenaerts, T., Arnout, J., Vermylen, J., and Hoylaerts, M. F. (2001) Congenital disorders of glycosylation Ia and IIa are associated with different primary haemostatic complications. *J. Inherit. Metab. Dis.* **24,** 477–492
26. Zdebska, E., Bader-Meunier, B., Schischmanoff, P. O., Dupré, T., Seta, N., Tchernia, G., Kościelak, J., and Delaunay, J. (2003) Abnormal glycosylation of red cell membrane band 3 in the congenital disorder of glycosylation Ig. *Pediatr. Res.* **54,** 224–229
27. Lübke, T., Marquardt, T., von Figura, K., and Körner, C. (1999) A new type of carbohydrate-deficient glycoprotein syndrome due to a decreased import of GDP-fucose into the Golgi. *J. Biol. Chem.* **274,** 25986–25989
28. Cantagrel, V., Lefeber, D. J., Ng, B. G., Guan, Z., Silhavy, J. L., Bielas, S. L., Lehle, L., Hombauer, H., Adamowicz, M., Swiezewska, E., De Brouwer, A. P., Blümel, P., Sykut-Cegielska, J., Houliston, S., Swistun, D., Ali, B. R., Dobyns, W. B., Babovic-Vuksanovic, D., van Bokhoven, H., Wevers, R. A., Raetz, C. R., Freeze, H. H., Morava, E., Al-Gazali, L., and Gleeson, J. G. (2010) *SRD5A3* is required for converting polyprenol to dolichol and is mutated in a congenital glycosylation disorder. *Cell* **142,** 203–217
29. Fujita, N., Tamura, A., Higashidani, A., Tonozuka, T., Freeze, H. H., and Nishikawa, A. (2008) The relative contribution of mannose salvage pathways to glycosylation in PMI-deficient mouse embryonic fibroblast cells. *FEBS J.* **275,** 788–798